ГОДИШНИК НА УНИВЕРСИТЕТА ПО АРХИТЕКТУРА, СТРОИТЕЛСТВО И ГЕОДЕЗИЯ
СОФИЯ

Том Volume 51 2018 Брой Issue 4

ANNUAL OF THE UNIVERSITY OF ARCHITECTURE, CIVIL ENGINEERING AND GEODESY
SOFIA

Получена: 15.09.2017 г.
Приета: 03.01.2018 г.

ASSESSMENT OF FATIGUE DAMAGE ACCUMULATION IN SPLIT-X CONCENTRICALLY BRACED FRAMES

L. Raycheva[1], Tzv. Georgiev[2]

Keywords: *low-cycle fatigue, braced frames, experimental tests, cyclic damage accumulation*

ABSTRACT

The current paper presents a characteristic aspect of cyclic non-linear behaviour of steel concentrically braced frames with braces, intersecting into a floor beam (Split-X CBFs). Through experimental programme three test specimens of one-bay one-storey Split-X CBF with braces of H-cross section were tested under fully reversed cyclic constant amplitude loading. The experimental observations prove the development of a distinctive mechanism of damage accumulation in braces which is presented by sequence of characteristic stages.

The typical stages of the damage accumulation process are defined and energy-based criterion for low-cycle fatigue endurance is formulated. Progressive drop in the energy dissipation capacity of the structure is observed when the accumulated damage in braces reaches a specific stage. It corresponds to brace fracture due to significant accumulation of growing and alternating plastic strains and exhaustion of material ductility. Based on the experimental study, a numerical equation defining the relation between brace elongation and low-cycle fatigue endurance is formulated. A non-linear analysis case study and low-cycle fatigue checks are presented.

[1] Lora Raycheva, Eng. PhD Student, Dept. "Steel, Timber and Plastic Structures", UACEG, 1 H. Smirnenski Blvd., Sofia 1046, e-mail: raycheva_fce@uacg.bg, lora_dr@abv.bg
[2] Tzvetan Georgiev, Assoc. Prof. Dr. Eng., Dept. "Steel, Timber and Plastic Structures", UACEG, 1 H. Smirnenski Blvd., Sofia 1046, e-mail: cvgeorgiev_fce@uacg.bg

1. Introduction

Concentrically braced frames (CBFs) are traditional and popular system for seismic resistant design. Nowadays CBFs are widely implemented in single storey industrial frames, multistorey buildings and industrial engineering facilities. This system has proved its efficiency for lateral loads by providing sufficient stiffness and strength due to its complete truss action which is the main reason for its popularity. The dissipative behaviour of conventional CBFs is provided primarily by yielding of braces in tension and to a smaller extent by plastic rotation in buckled braces.

Provision of the demanded ductility is related to ensuring formation of predefined plastic mechanism that excludes concentration of plastic deformations in a single storey. In this regard Eurocode 8 requires limitation of the brace overstrength among all storeys and capacity design for all non-dissipative elements as to assure the formation of global plastic mechanism.

Scientific research in the field of inelastic cyclic behaviour of CBFs with different configuration of braces proves that the system energy dissipation capacity and the resultant plastic mechanism are highly sensitive to the configuration of braces within the braced frame as well.

Detailed research on the V-CBFs cyclic behaviour performed by *Khatib* et al. [5] reveals that the intended plastic mechanism and expected ductility of the system may be obstructed due to occurrence of intersecting beam bending. It is a result from the formation of unbalanced vertical force in post-buckling stage. This type of structural behaviour reflects in induction of supplementary and non-uniform deformations in the braces and eventually – in reduction of structural ductility and brace endurance.

An inherent tendency for non-uniform distribution of deformations is attributed to the Split-X configuration of CBFs. It is related to the presence of horizontal inertia force in the intermediate level where braces intersect, which results in requirement for greater lateral stiffness and strength of the lower level of the Split-X CBF. *Lacerte* and *Tremblay* [6] also prove the propensity of Split-X CBF to concentrate inelastic deformations in a single storey and the subsequent reduction of system ductility and brace endurance. Authors propose criteria for homogeneous plastic deformations distribution, achieved by limitation of the ratio of lateral force resistance of two adjacent storeys. Further investigations on Split-X CBFs are performed by *Jay Shen* et al. [7, 8] in their numerical study of six- and twelve-storey CBFs. Authors confirm the tendency for concentration of inelastic deformations in a single storey and prove the effect of splitting beam stiffness on the type of resultant plastic mechanism and the uniformity of plastic deformations along the building height due to presence of unbalance forces in elasto-plastic and post-buckling stage. Most of the authors are in full agreement about the major influence of brace slenderness on Split-X CBFs behaviour.

Comprehensive research regarding the influence of splitting beam stiffness on the seismic response of chevron CBFs is performed by *D'Aniello* et al. [9]. Authors highlight the relation between the beam-to-bracing stiffness ratio and global and local performance parameters influencing the seismic response of chevron V-CBFs. As a result of the extensive numerical parametric study, they propose analytical expressions for controlling the local brace ductility demand and the plastic mechanism at different performance levels.

Experimental programme, conducted in UACEG, Bulgaria in 2011 (*Georgiev*, [10]) has shown that non-homogeneous plastic deformations may be observed in single storey X-CBFs with diagonals that intersect into a horizontal splitting stud due to the non-concurrent buckling of the two compressed braces from a couple. *Georgiev* and *Raycheva*, [11] prove the significance of the interaction between splitting beam and column bending stiffness for the

regularity of plastic deformations distribution in CBFs with modified braces. An analytical model is proposed for defining the sufficient splitting beam and column stiffness.

The review of the experimental and numerical investigation on the inelastic behaviour of Split-X CBFs proves the tendency of this system for non-uniform distribution of deformations along the building height and concentration of plastic strains in few braces. Plastically engaged diagonals suffer severe concentration of plastic deformations in their mid-length section when exposed to reverse cyclic loading which leads to premature fracture of the element. Being the main dissipative elements in the CBF system, the abovementioned premature brace fracture results in reduced ductility of the system and thus raises the issue for proper evaluation of the low-cycle fatigue endurance of the braces.

Extensive research on the types of failure mechanism due to reversed plastic strains in steel material is performed by *Nip* et al. [12]. The author defines a variation of typical low-cycle fatigue (LCF) named extremely low-cycle fatigue (ELCF). The mechanism of cyclic failure of the tested standard steel specimens is related with the type of observed fracture surfaces. ELCF failure mechanics is explained with interaction of material ductility exhaustion and fatigue crack development and is attributed to failure at number of cycles lower than 100. LCF and ELCF failure mechanism may be found characteristic for Split-X CBFs due to the typical non-uniformity of the distribution of deformations along the building height and the specificities of a single brace cyclic behaviour. It is described by the interaction of member plastic elongations and section strains due to bending and local buckling in the mid-zone of the braces. This specific mechanism of brace failure in Split-X CBF, was observed during the experimental programme, conducted in UACEG in 2016 and described in detail in the current paper.

Together with material cyclic tests, researchers point the importance of performing cyclic tests of assemblage of structural elements where the specificities of the assemblage behaviour and the connection used affect the mechanism of strain distribution and the overall process of damage accumulation. *Krawinkler* et al. [13] proposes recommendations for experimental studies on the damage accumulation and fatigue life prediction of steel components that lay down in the basics of ATC-24 [2].

In this regard, the main objective of authors' research is the assessment of the mechanism for damage accumulation in braces with built-up welded "H-shape" cross section during full reversal cyclic constant amplitude tests. Observations on failure development due to cyclic loading and its influence on the overall ductility of the Split-X CBF are drawn. Criterion for assessment of accumulated damage in braces is proposed as well as a non-linear analysis case study and damage index checks are presented in the current paper.

2. Experimental Programme

In the scope of the conducted experimental programme three test specimens of one-bay one-storey concentrically braced frame with braces, intersecting into a splitting beam were designed, manufactured and tested. CBF specimens are 4000 mm in height and 3000 mm column bay width. Braces are designed of welded "H-shape" cross section and steel grade S235JR. The non-dimensional slenderness is $\bar{\lambda} = 1,28$. Table 1 summarizes the cross-sections and steel-grade used for the elements of each specimen. The cross sections of the braces are designated by abbreviation that should be read as follows: F80/5 (flange width 80 mm and thickness 5 mm) и W120/5 (web height 120 mm and thickness 5 mm). Columns were oriented with their minor axes in the frame plane while the beams were traditionally oriented with its major axis in the plane frame. Splitting beams are designed in two variations of the cross

section – as stiff and flexible. All the connections between elements are realized as pinned with the exception of the connection between the splitting beam and columns which can be classified as partially rigid. The actual brace yield stress ($f_{y,act}$) was defined through standard tensile test.

Table 1. Specimen elements sections and steel grade

	Specimen 1	Specimen 2	Specimen 3
Columns	HEA320/S275	HEA320/S275	HEA320/S275
Top Beam	HEA200/S275	HEA200/S275	HEA200/S275
Splitting Beam	IPE200/S275	HEA240/S275	IPE200/S275
Braces	H(F80/5,W120/5)* /fy,act = 303 MPa	H(F80/5,W120/5)* /fy,act = 303 MPa	H(F80/5,W120/5)* /fy,act = 303 MPa

The tests were conducted by applying controlled displacement at the top of the frame by a hydraulic actuator. The test setup is illustrated in Fig. 1.

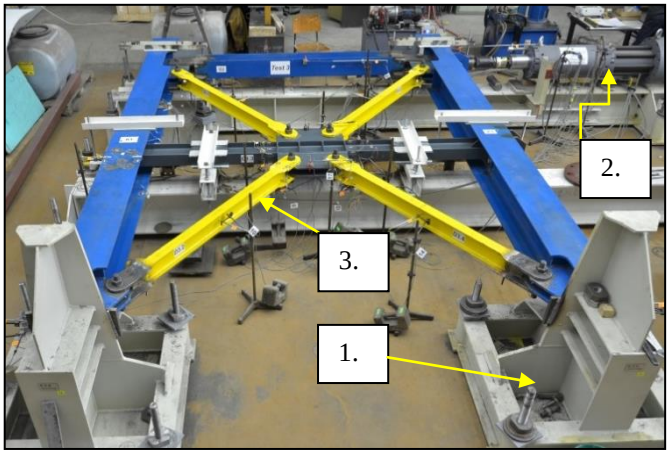

Figure 1. Experimental setup

1. Supporting stand; 2. Hydraulic actuator; 3. Test specimen

Each of the specimens was tested by two protocols: monotonically increasing applied top displacement with magnitude of 100 mm (Test 1) and statically applied top displacement in fully reversal symmetrical cycles with constant amplitudes (Test 2). Amplitudes of 85, 115 and 140 mm for Specimen 1, 3 and 2, respectively were used. The significant visible damage is reported during each test at every cycle. Distinctive displacements and strains were registered by strain gauges (SGs) and inductive displacement transducers (ITs), installed at characteristic sections. The adopted loading protocol is in accordance with the test purpose and meets the recommendations for experimental studies on the damage accumulation and life prediction of steel components, prescribed by *Krawinkler* et al. [13] and ATC-24 [2].

3. Mechanism of Damage Accumulation

Observations from the cyclic constant-amplitude test (Test 2) revealed the existence of distinctive process of damage accumulation in the brace mid-section. The observed mechanism is represented by sequence of seven characteristic stages that are defined and illustrated by photos in Fig. 2. Each of the defined stages is described by the following:

1. Occurrence of local buckling of one of the flanges (top or bottom) at the concave side of the buckled brace. The buckled zones are realized as local cumulative strain concentrators. Together with local buckling strains, bending strains from global brace buckling are accumulated in the same mid-section. The interaction of global and local effect of strain accumulation is the main failure mechanism, predetermining the brace cyclic endurance.

2. Occurrence of local buckling of both flanges at the concave side of the buckled brace.

3. Occurrence of local buckling of one of the flanges at the convex side of the brace.
The buckling of the outer fibres from the convex side was observed during brace elongation. These fibres have been plasticised and elongated in bending due to the post-buckling brace behaviour. Following the load reversal, the diagonal goes straight and the curvature in the middle decreases. Being already elongated, the outer fibres have to accommodate the new geometry and thus plate buckling develops.

4. Surface crack initiation at the flange local buckling wave of maximum curvature.
The subsequent stages 5, 6 and 7 develop rapidly in the range of up to two cycles.

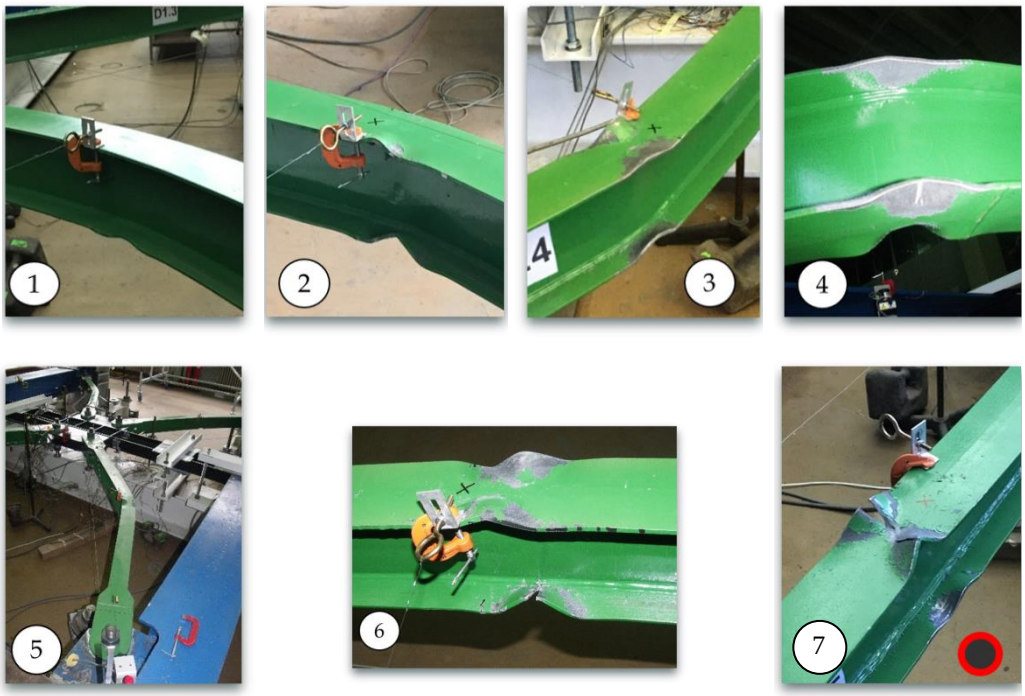

Figure 2. Stages of damage accumulation in braces during reversal cyclic test

5. Concentration of inelastic deformations and formation of sharp bend in the brace web.

As illustrated in Fig. 3, the brace deformed shape can be approximated with two straight studs, joined by a segment with semi-constant radius. After initiation of crack in the flanges, the brace global bending deformations concentrate in the brace web. This reflects in transformation of the deformed shape of the brace to one, approximated with two intersecting straight studs.

6. Tearing of one flange along its width and propagation of the crack towards the web.

7. Occurrence of flange tearing of other brace flange.

A variance of the type of local buckling, described in Stage 1 was observed for the brace that buckles second from the compressed pair of diagonals. The observed deformed shape is characterized with bending of the flange along large length, forming sort of "macro-buckling-wave". The described brace deformation is presented in Fig. 3.

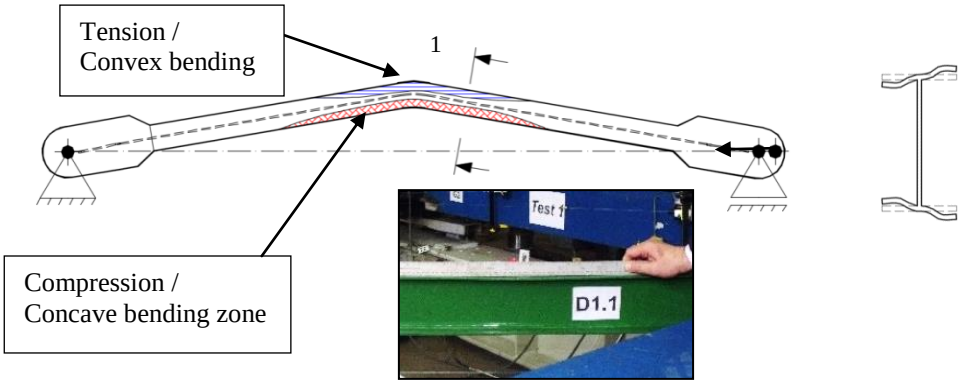

Figure 3. Variance of brace local buckling, formation of 'macro-buckling-wave'

During the performed constant amplitude cyclic test, total brace fracture was not met. The brace web preserved its integrity. The web tearing was achieved in the end, after applying larger displacement than the adopted constant amplitude of lateral displacement.

The observed stages develop in the exposed sequence for a single brace but among the four braces in a specimen, their occurrence is asynchronous. This may be attributed to the non-concurrent buckling of both braces from a couple, caused by insufficient bending stiffness of the splitting beam and/or different initial imperfections of braces. This matter is studied in detail by *Georgiev et al.* [11, 14].

4. Assessment of Accumulated Damage in Braces

4.1. Energy-Based Approach

The effects of damage accumulation are assessed through energy-based approach adopted in the research of *Castiglioni* et al. [15] & *Bernuzi* et al. [16]. It is related to definition of "cyclic energy dissipation reduction factor" (α_i), represented by the ratio of the amount of dissipated energy during the current cycle (E_i) and the amount of dissipated energy during a reference cycle (E_b) (eq. (1)):

$$\alpha_i = \frac{E_i}{E_b}. \quad (1)$$

Considering the characteristic hysteresis response of CBFs, the first cycle in which the distinctive pinching effect occurs is regarded as a reference cycle. The value of the defined criteria at each cycle of the applied load historey for the test of Specimen 1 is illustrated in Fig. 4.

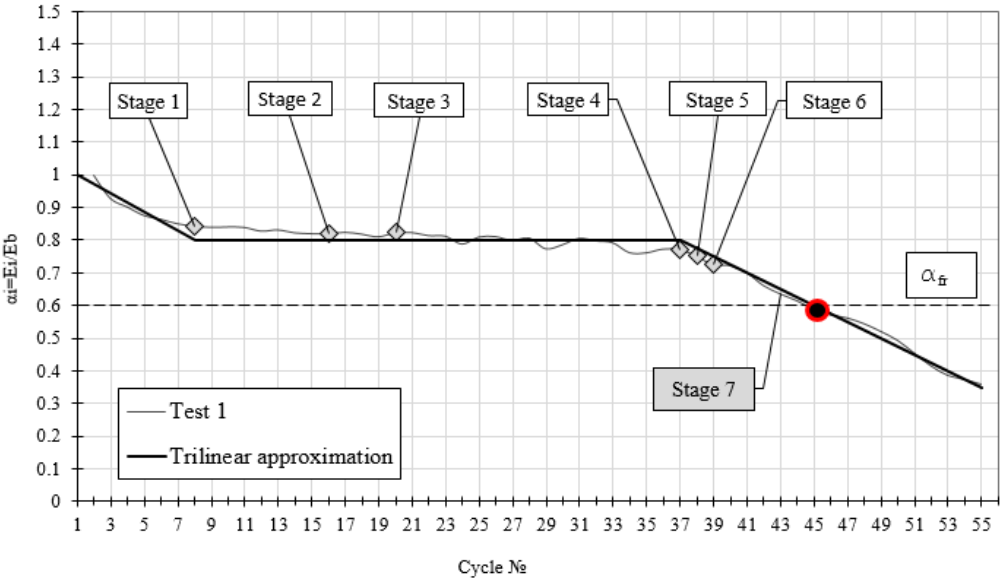

Figure 4. Relation between the cyclic energy dissipation reduction factor and the number of cycles for Specimen 1

Three distinctive ranges can be distinguished. The first is characterized by a rapid drop of dissipated energy, a plateau of constant energy dissipation capacity and a subsequent rapid drop. The rapid drop appears after the first initiation of surface crack at a brace flange. The last branch may be related to a drop of system energy dissipation capacity due to significant amount of accumulated damage.

Criterion for significant loss of dissipated energy due to cyclic damage accumulation in braces is proposed by defining a lower bound of the "cyclic energy dissipation reduction factor" $\alpha_{fr} = 0,6$. Similar approach is used by *Castiglioni* and *Calado* [16]. This value of α_{fr} is derived by a reduction coefficient $b = 0,8$ by which the value of α_i at the plateau is multiplied. The adoption of $b < 1,0$ is associated with the observed ductile mechanism of brace fracture and the type of fracture surface. The observed fracture surface is indicative for fractures at extremely low-cycle fatigue range (ELCF). Referring to the research on the cyclic steel fracture mechanics and fracture surfaces, performed by *Nip* et al. [12], ELCF is related to fracture due to interaction of steel ductility exhaustion and fatigue crack development. The observed surface associated with this type of failure is described as "mixed" of ductile and fatigue damage surface. According to cyclic test observations of steel material, ductile fracture leads to relatively uneven surface that is dull in appearance, often exhibiting cup-and-cone profile. On the other hand fatigue failure is characterized by a series of 'beach' marks that

indicate the progressive advancement of a fatigue crack. The fracture surface of tested specimens was inspected visually. It might be said that it is characterised by fatigue surface at the crack initiation areas and ductile surface where the crack propagates.

Comparison of the cyclic energy dissipation reduction factor historeys for the performed three cyclic constant amplitude tests reveals the similarities between them and shows the development of universal mechanism for damage accumulation in braces of welded H-cross section. Moreover, it can be noticed that the slope of the falling range after fracture initiation is almost constant.

It is evident from Fig. 5 and Fig. 6 that a trade-off exists between the number of cycles to a specific stage of accumulated damage and the value of the applied load amplitude. This relation complies with the Palmgren-Miner rule (*Balio et al.* [17]).

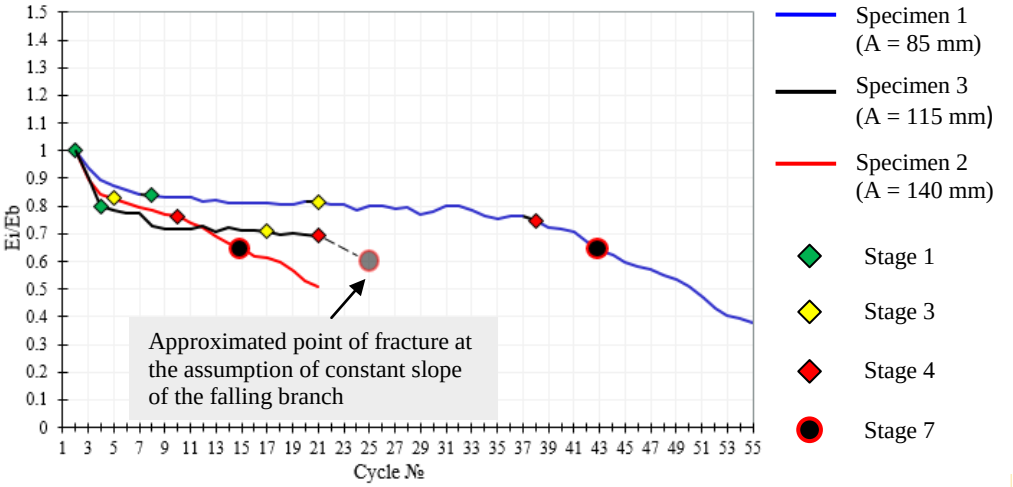

Figure 5. Cyclic energy dissipation reduction factors for the three cyclic constant – amplitude tests

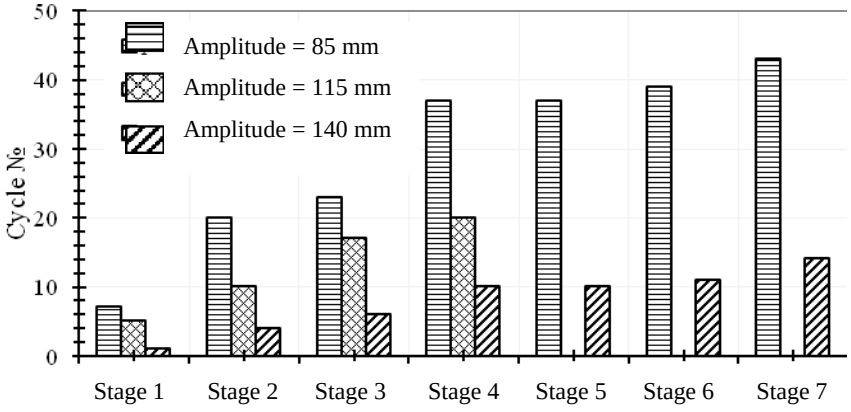

Figure 6. Relation between the numbers of cycles at first occurrence of particular stage of accumulated cyclic damage for the three tests

4.2. Analytical Assessment of Brace Cyclic Endurance

In order to assess the degree of accumulated damage in H-braces of Split-X CBF due to real ground motion records, an analytical equation is defined:

$$\delta(N) = 60 - 30\log(N). \quad (2)$$

The proposed equation (2) relates the axial deformation amplitude of a single brace, δ corresponding to the number of cycles to failure, N. It is derived using the experimental results from the performed three cyclic constant amplitude tests of single-storey Split-X specimens. It relates the number of cycles to fracture defined by the limit value α_{fr} and the amplitude of the applied axial displacement. The proposed formula (2) was defined by shifting of the experimentally observed relation to the safe side with deviation of 0,834. The following assumptions are made when deriving equation (2):

- linear relation between global (elongations/shortenings) and local (strains) brace deformations (*Ballio* and *Castiglioni* [17]);
- validity of equation (2) for brace axial deformation amplitudes not less than the axial deformation at first yield: $d > dy$.

The experimental and numerical relations are illustrated in Fig. 7. If the experimentally formulated relation from Fig. 7*a* is presented in log-log format, the Coffin-Manson linear relation for the low-cycle fatigue life is obtained (Fig. 7*b*). The fatigue ductility exponent may be assessed with value of 0,47. Previous test research by *Castiglioni* and *Calado* [15] has demonstrated values in the range of 0,5 – 0,7. The similarity between these values and the values derived by the current tests proves the adequacy of the experimentally obtained relation. It is evident from Fig. 7*a* that Eqn. (2) gives quite conservative values, leading to 60 cycles to fracture at amplitude equal to the brace yield displacement in tension (δy = 5 mm). This value is considered conservative but acceptable for design checks. At that stage of the study, more precise equation would not be drawn since it requires more tests and variation of more parameters as length, slenderness, cross-section sizes and classes.

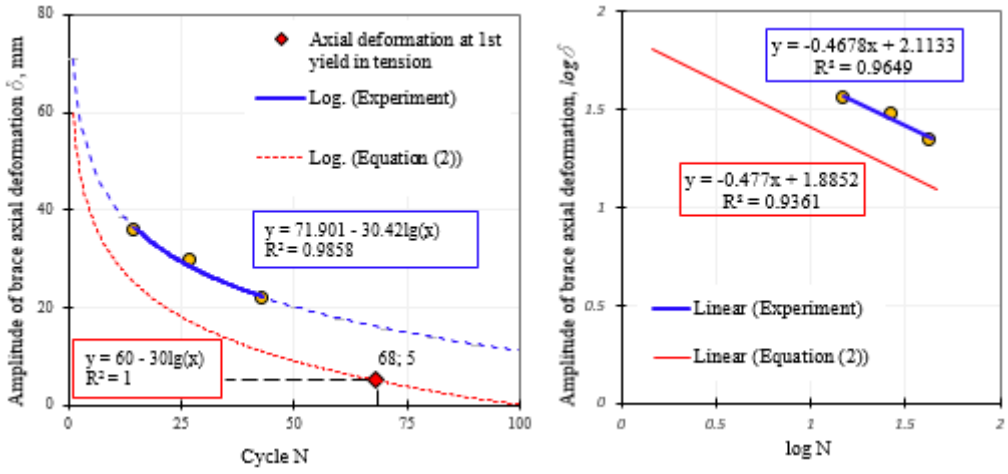

a) *b*)

Figure 7. Experimental and numerical relation between brace axial deformation amplitude at fracture and number of cycles to fracture *a*) absolute values *b*) log-log format

After processing of the test results, the relation between a single brace axial deformation and the horizontal roof displacement of the test specimen is derived with the assumption for equality between the axial deformation and degree of cyclic damage accumulation of both braces in a pair (Eqn. (3)). During the performed tests this assumption was not fully met – braces observed different stages of accumulated damage. In this point of view, the conservatism in the proposed Equation (2) is justified, regarding effects from non-uniformity of the plastic strains and the stages of accumulated damage between the two braces from a pair.

$$\delta = 0,85\Delta\cos\alpha/2. \tag{3}$$

Similar equation is proposed by *Georgiev* [10], where instead of 0,85, coefficient 0,90 is promoted.

4.3. Validity of the Proposed Equation with Respect to Brace Slenderness

In order to assess the validity of the proposed Eqn. (2), parametric study was conducted in SeismoStruct v7.0 [18]. A set of eight fibre FE models of a single brace is generated. The modelling of the brace is performed in compliance with the recommendations of *D'Aniello* et al. [19]. Buckling of the brace is provoked by imposing an initial geometric imperfection of 0,50% in the mid joint of the brace. The cross section of the braces is H-shaped and meets the requirements of Eurocode 3 [4] for class 1. The brace slenderness is varied. Braces with non-dimensional slenderness in the range of 0,6 – 2,25 were investigated. Static nonlinear analysis is performed for each of the models. The applied load is cyclic fully-reversed axial displacement with constant amplitude.

The maximum, minimum and mean strain and the strain range for the most strained fibre of the brace cross section (the upper left in the case) are plotted in relation to brace slenderness (Fig. 9). The historey of strains for each model is plotted in Fig. 8.

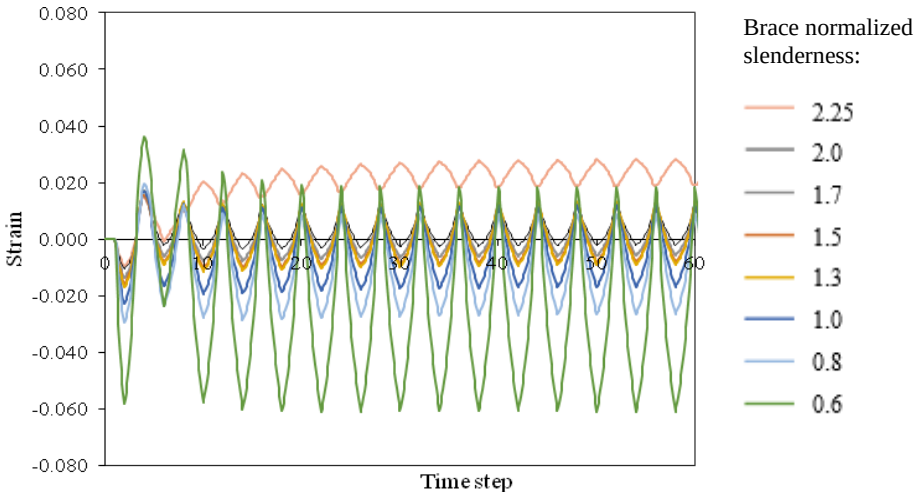

Figure 8. Historey of strains in the upper left fibre of the mid-section of single H-brace

It can be noticed that for brace slenderness in the range of 1,00 – 2,00 (the hatched area in grey), the evaluated strains may be regarded as constant. This proves the validity of the assumption for linear relation between strain and axial deformation of a brace and the validity of the proposed Equation (2) in the range of non-dimensional brace slenderness 1,00 – 2,00.

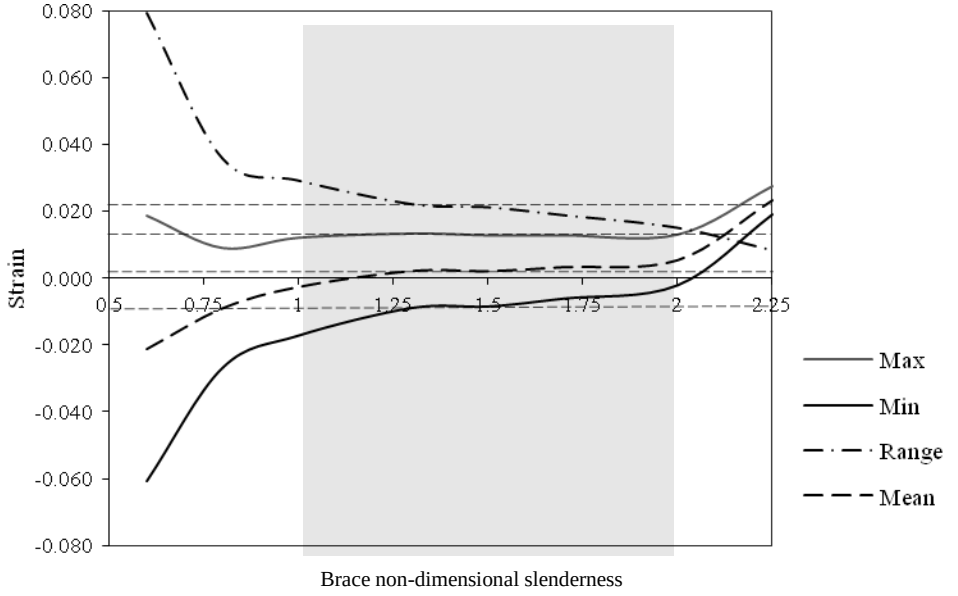

Figure 9. Variation of strains with change of non-dimensional slenderness of a single H-brace

5. Case Study

The application of the proposed Equation (2) for assessment of accumulated damage in braces of two-storey Split-X CBF is illustrated through a case study by performing a series of dynamic time-historey analysis.

5.1. Geometry and General Assumptions

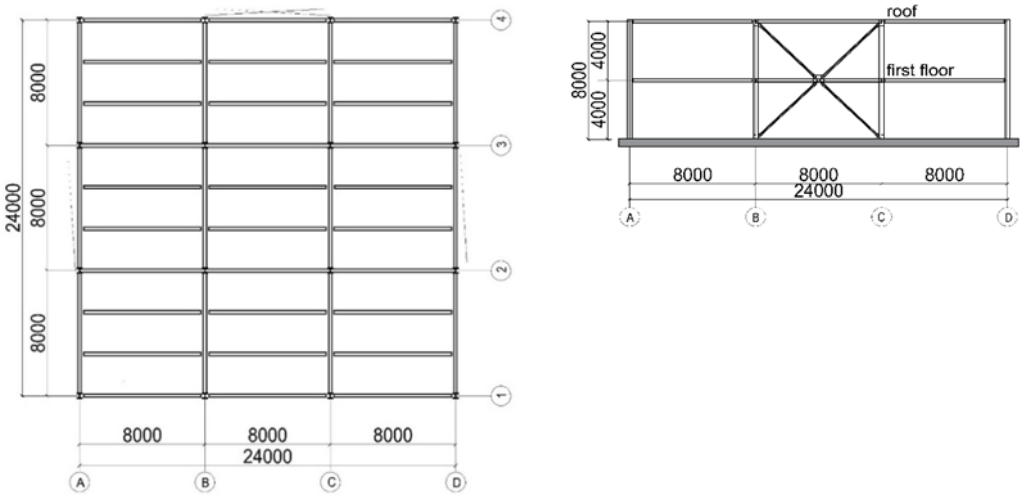

Figure 10. 2D building frame and building plan

The case study presented hereafter is based on a plane Split-X CBF-MB frame extracted from a two-storey building, Fig. 10. The frame consists of three 8 m bays with nominally pinned beam-to-column joints and pinned column bases. The Split-X CBF systems are located as shown in Fig. 10. Hot rolled HEA profiles and IPE profiles for columns and floor beams are used. Composite action with the concrete slab is not considered (*Georgiev* et al. [20]).

Table 1. Cross sections and steel grade used for the Split-X CBF elements

	Split-X CBF			Building frame		
Storey	Braces	Columns	Splitting beams	External columns	Internal columns	Beams
1	F180.12W160.8/ S235	HEB 300 / S275	HEB 300/ S275	HEA 200/ S275	HEA 240/ S275	IPE360 HEA400/ S275
2	F150.10W160.8/ S235	HEB 300 / S275	HEB300 /S275	HEA 200/ S275	HEA 240/ S275	IPE300 HEA340/ S275

The design of the presented building is conducted for vertical loads and for seismic design situation. The structural linear elastic model was formed using beam finite elements. Split-X CBF members are designed and modelled as follows. Split-X CBF columns are continuous. All joints between splitting beams and columns and the joints between beams and columns are assumed nominally pinned. The elements simulating the braces are defined by constant H-shape cross-section and joined to the frame by simple pin connections. Split-X CBF column bases were designed and detailed as pinned, which is considered the most practical approach for this type of system. Diaphragm action of floor and roof concrete decks is simulated by diaphragm constraint.

The elastic analysis performed in the case study is based on model with all frame diagonals included. At first glance, this can be interpreted as diverting from the Eurocode 8 [3] postulates. On the other hand, Eurocode 8 keeps silent about Split-X CBFs. The authors have preferred to interpret the system as a combination of V- and Λ-CBFs for which Eurocode 8 recommends modelling of both diagonals. It is worth commenting that the current design follows the requirements of AISC-2010 [1] for design of SCBFs, where it is stipulated that the model should include both tension and compression braces. The characteristics of the design response spectrum used in the multi-modal response spectrum analysis are presented in Table 3.

Table 3. Characteristics of the design response spectrum for elastic analysis

Design response spectrum for elastic analysis	Type 1
Reference peak ground acceleration	$a_{g,R}$ = 0,30 g
Importance class II (Ordinary building)	γ_I = 1,0
Ground type	B (T_B = 0,15 s, T_C = 0,50 s)
Behaviour factor *q (first guess of the authors)*	4,0
Damping ratio	5%

5.2. Nonlinear Dynamic Analysis

5.2.1. Structural Model

In order to demonstrate the application of Equation (2) and to assess the state of accumulated damage in braces of two-storey Split-X CBFs exposed to real strong ground

motion, a series of fourteen nonlinear dynamic analyses were performed. The finite element model for dynamic analysis is created using the software SeismoStruct v.7. Nonlinear hysteresis steel material model of Menegotto-Pinto is adopted and the specific parameters used are calibrated to experimental results. Inelastic force-based fibre elements are used for modelling Split-X CBF elements. Braces are modelled as described in point 4.3 of the current paper. P-Delta effects are taken into account by introducing a leaning column. Overview of the structural model and properties of the adopted material model are presented in Fig. 11.

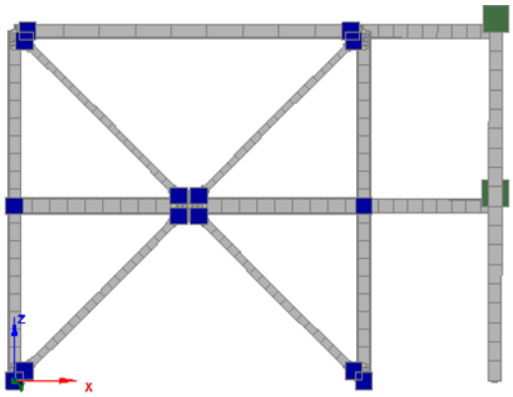

a)

Modulus of elasticity (kPa)	210 000 000
Yield strength (kPa)	302 000
Strain hardening parameter	0,008
Transition curve initial shape parameter	19,9
Transition curve shape calibrating coefficients:	
A1	18,6
A2	0,01
Isotropic hardening calibrating coefficients:	
A3	-0,011
A4	2,00

b)

Figure 11. Split-X CBF FE model for dynamic analysis *a*) properties of adopted steel hysteresis Menegotto-Pinto model *b*)

5.2.2. Ground Motion Records

Non-linear dynamic analyses (time historey with direct integration) were performed. The examined braced frame was subjected to a suite of ground motion records obtained from Far-Field-Record set with PGA not much larger than 0,3 g. This set was considered appropriate for obtaining the time-dependent response of the structure and in particular the braces. The set includes fourteen real records of the strongest horizontal ground motions from the PEER NGA database and refers to sites located greater than or equal to 10 km from fault rupture, all having magnitude more or equal to 6,5. Adjustment of the selected strong ground motion records was achieved through the software SeismoMatch [21], which is able to process ground-motion records so that their spectral acceleration response matches target response spectrum (TRS). Matching of the records was based on the Eurocode 8 rules for artificial accelerograms. The adjusting process was performed for all of the 14 signals. The criterion of Eurocode 8, stating that in the range of periods between $0{,}2T_1$ and $2T_1$ no value of the mean spectrum should be less than 90% of the corresponding value of the elastic response spectrum, was fulfilled. List of selected strong ground motion records and their basic characteristics is shown in Table 4.

Table 4. List of selected strong ground motion records

№	Earthquake			Recording Station		Recorded Motions		Matched Motions	
	M	Year	Name	Scale factor	Name	PGA max (g)	PGV max (cm/s)	PGA max (g)	PGV max (cm/s)
1	7,1	1999	Hector Mine, USA	1,2	Hector (90)	0,34	42	0,56	37
2	6,9	1995	Kobe, Japan	1,0	Kakogawa (CUE90)	0,34	42	0,35	32
3	7,5	1999	Kocaeli, Turkey	1,0	Duzce (270)	0,35	11	0,52	31
4	6,9	1989	Loma Prieta, USA	1,2	090 CDMG	0,37	45	0,34	55
5	6,5	1987	Superstition Hills, USA	1,0	Poe Road (temp)	0,28	10	0,42	32
6	7,6	1999	Chi-Chi, Taiwan	0,8	TCU 045	0,36	22	0,52	43
7	6,5	1976	Friuli, Italy	1,0	Tolmezzo (000)	0,35	22	0,48	37
8	6,7	1994	Northridge, Beverly Hills	1,5	Northr/MUL009	0,42	59	0,47	40
9	6,5	1979	Imperial Valley, Delta	1,0	Impvall/H-DLT352	0,35	33	0,35	22
10	7,3	1992	Landers, Coolwater	1,2	Landers/CLW-LN	0,28	31	0,40	47
11	7,4	1990	Manjil, Iran	1,2	Manjil/184057	0,41	59	0,41	59
12	6,6	1971	San Fernando, LA – Hollywood Stor	1,0	SFERN/PEL180	0,21	19	0,39	47
13	6,4	1983	Coalinga, Cantua Creek School	1,0	Coalinga.H_H-CAK270	0,22	5	0,37	32
14	7,9	2002	Denali_Alaska, R109(temp)	1,0	RSN2111_Denali_ R109360.AT2	0,11	2,33	0,53	33

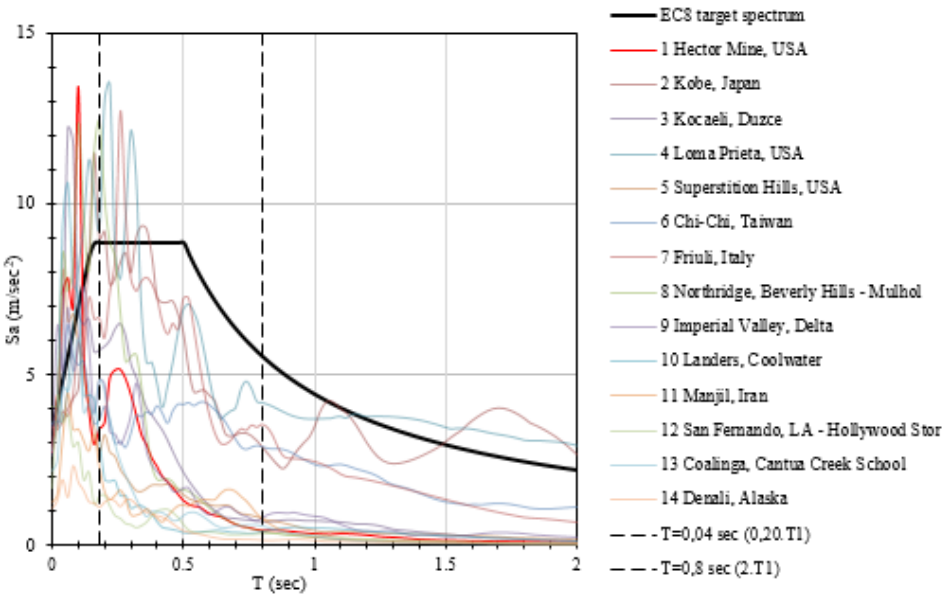

Figure 8. Response spectrums of the recorded accelerograms and Target RS

As TRS the Eurocode type 1 Response Spectrum (RS), based on PGA 0,3 g and Soil Type B is used. Fig. 12 illustrates the RSs of the recorded accelerograms and the TRS. The Mean Matched RS of the matched accelerograms, the TRS and the 90% TRS are shown in Fig. 13.

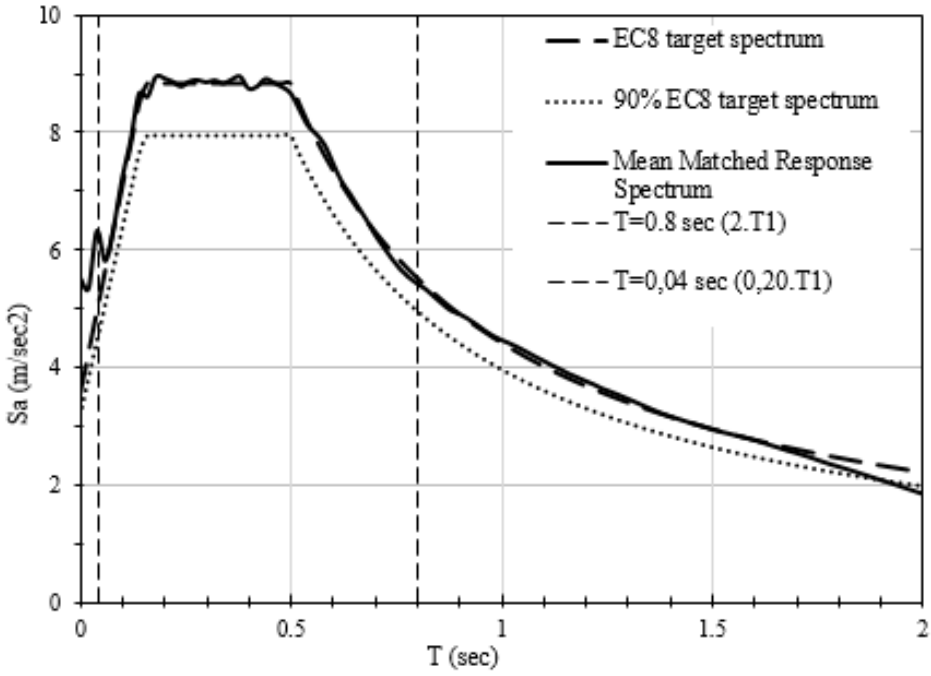

Figure 9. Target Response Spectrum, 90% Target RS and Mean Matched RS

5.2.3. Accumulated Damage in Braces

In order to make assessment of the stage of accumulated damage in braces, Eqn. (2) is used. The time historeys of brace axial elongations and shortenings are extracted from the SeismoStruct nonlinear model output for the inelastic force-based fibre elements. Number of cycles was counted by rainflow method, ignoring all cycles with amplitudes less than 5 mm. The former was adopted since the proposed formula is very conservative for amplitudes less than 5 mm (brace yielding axial deformation). Based on Equation (2) and the Miner's rule, damage indexes were calculated and reported in Table 5 for each of the signals. Damage indexes are calculated following the Palmgren-Miner rule presuming linear damage accumulation model and using Equation (4). Following the accepted definition of failure (point 4.1), *DI* = 1,0 is regarded as brace endurance exhaustion and flange tearing.

$$DI = \sum_{i=1}^{k} \frac{n_i}{N_i}, \tag{4}$$

where N_i is the number of cycles at which failure would occur in case of ith strain level;

n_i is the counted number of cycles carried out at strain level *i*;

k is the total number of strain levels of constant amplitude.

Table 5. Damage indexes

Seismic Record	Damage Index
1. Hector Mine	0,138
2. Kobe	0,133
3. Kocaeli	0,150
4. Loma Prieta	0,148
5. Superstition Hills	0,130
6. Chi-Chi	0,075
7. Friuli	0,179
8. Northridge	0,076
9. Imperial Valley	0,192
10. Landers	0,146
11. Manjil	0,154
12. San Fernando	0,191
14. Coalinga	0,144
15. Denali	0,079

It is evident from Table 5 that in all cases the damage indexes appear well below one, demonstrating very low degree of accumulated damage in braces. This proves the good endurance of braces of the examined H-cross section. It is worth noting that the presented study corresponds to Significant Damage Limit State. If the study is extended to Near Collapse Limit State, the brace Damage Index will increase.

6. General Observations from the Performed THA and Experimental Tests

Comparing the endurance of conventional braces with tubular cross section to the one with the examined H-cross section, the superiority of the latter may be stated firmly. Despite the detrimental mechanism of developing plastic strains in braces with H-cross section, their global integrity is kept until high number of cycles (N = 15) for interstorey drift ratio of 3,5%. This is attributed to the lack of concentration of local plate buckling in the brace web. Unlike H-braces, the conventional tubular braces exhibit sudden fracture due to low-cycle fatigue at a relatively low number of cycles and at low drifts.

Cyclic experimental test of two-storey CBF specimen with tubular brace sections had been performed by *Uriz and Mahin* [23]. The braces have passed 6 cycles of 0,15% drift, 4 cycles of 0,5% drift. The major fracture of the braces has been observed at the first cycle of 1,38% drift. Authors *Uriz & Mahin* describe the mechanism for damage accumulation in tubular braces with four stages:

- gradual tearing of the corners of the tubes perpendicular to the longitudinal axis of the brace at a location where the crest of major local buckle had previously formed on the most compressed side of the brace;
- sudden merging of the corner tears across the entire side of the brace;
- gradual growth of this crack across the depth of the section;
- sudden rupture of the entire section.

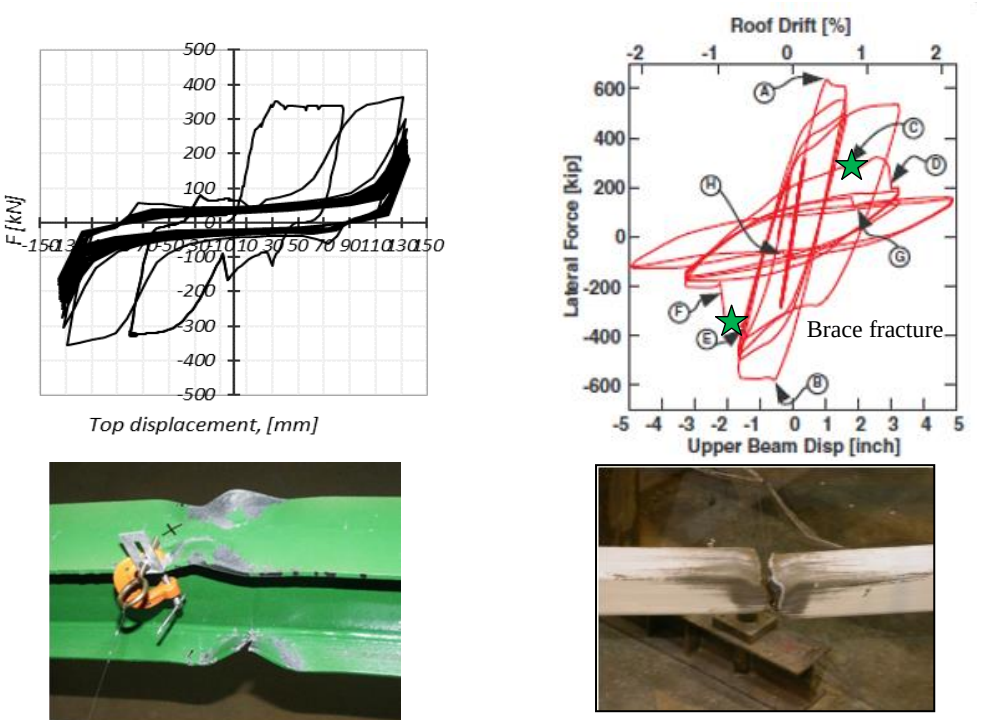

a) Georgiev, Tzv., Raycheva, L., UACEG, Sofia, Bulgaria 2016 [22]

b) Uriz, P., Mahin, S., University of Berkley, California, 2002 [23]

Figure 10. Comparison of hysteresis response of CBFs with braces of H-section *a*) and conventional tubular cross section *b*)

The described process is regarded as more unfavourable than the observed one during the test of CBF with H-braces. This is visible also from the global hysteresis response of the CBF systems and is illustrated in Gig. 14. In the opinion of the authors of this article, diagonals for CBFs with open H-shaped sections have significant advantages and can be successfully applied for seismic resistant design of buildings in areas of high seismicity.

7. Conclusion

The performed cyclic constant amplitude tests on Split-X CBFs reveal a distinctive mechanism of damage accumulation in braces. The observed system behaviour proves the good endurance of braces with built-up welded H-cross sections, described by lack of sudden brace fractures, development of stable gradual cumulative damage mechanism and lack of total brace fracture. This satisfactory cyclic behaviour may be attributed to the shape of braces cross-section – welded H-shape that in comparison with tubular cross sections, exhibits superior endurance.

The defined criteria for assessment of the number of cycles related with significant drop of Split-X energy dissipation capacity and the proposed numerical equation for assessment of the degree of accumulated damage for cyclic load with variable amplitude of a single brace is

applicable in assessment of Split-X premature failure of braces when performing dynamic analysis with real strong ground motions.

Acknowledgements

Authors would like to express their acknowledgements to The Research, Consultancy and Design Centre of the University of Architecture, Civil Engineering and Geodesy, (ЦНИП) and the Ministry of Education and Science (MOH) for the financial support, enabling the realization of the experimental programme. Without their financial support, the current study would not have been carried out.

REFERENCES

1. ANSI/AISC 341: 2010, Seismic Provisions for Structural Steel Buildings.

2. ATC-24 (Applied Technology Council) (1992), Guidelines for Cyclic Seismic Testing of Structural Components of Steel Structure, Krawinkler H.

3. Eurocode 8: Design of structures for earthquake resistance – Part 1: General rules, seismic actions and rules for buildings; EN 1998-1:2004.

4. EN1993-1-1, Eurocode 3: Design of steel structures – Part 1-1: General rules and rules for buildings. Brussels: Comitee Europeen de Normalisation (CEN); 2003.

5. *Khatib, I., Mahin, S. and Pister, K.* Seismic Behavior of Concentrically Braced Steel Frames, Report No. UCB/EERC – 88801, *University of California,* Berkeley, 1988.

6. *Lacerte, M., Tremblay, R.* "Making Use of Brace Overstrength to Improve the Seismic Response of Multistorey Split – X Concentrically Braced Steel Frames", Canadian Journal Civil Engineering 33: 1005-1021 (2006), NRC Canada, 2016.

7. *Shen, J., Wen, R., Akbas, B.* "Mechanisms in Two-Storey X-Braced Frames", Journal of Constructional Steel Research 106 (2015) 258-277, 2014.

8. *Shen, J., Wen, R., Akbas, B., Doran, B., Uckan, E*. "Seismic Demand on Brace-Intersected beams in Two-Storey X-Braced Frames", Engineering Structures 76 (2014) 295-312, 2014.

9. *D'Aniello, M., Costanzo, S., Landolfo, R.* "The Influence of Beam Stiffness on Seismic Response of Chevron Concentric Bracings", *Journal of Constructional Steel Research* 112 (2015) 305-324, 2015.

10. *Georgiev, Tzv.* "Study on Seismic Behaviour of "X" CBFs with Reduced Diagonal Sections", *PhD Thesis (in Bulgarian), UACEG, Sofia, 2013.*

11. *Georgiev, Tzv., Raycheva, L.* "Influence of Splitting Beam and Column Stiffness on CBFs Ductile Behaviour", EUROSTEEL 2017, September 13–15, Copenhagen, Denmark, 2017.

12. *Nip, K., Gardner, L., Davies, C., Elghazouli, A.* "Extremely Low Cycle Fatigue Tests on Structural Carbon Steel and Stainless Steel", Journal of Constructional Steel Research 66 (2010) 96-110, 2010.

13. *Krawinkler, H., Zohrei, M., Lashkari-Irvani, B., Cofie, N., Hadidi-Tamjed, H.* "Recommendations for Experimental Studies on the Seismic Behavior of Steel Components and Materials", The John A. Blume Earthquake Engineering Center, Department of Civil Environmental Engineering, Report No. 61, 1983.

14. *Georgiev, Tzv., Zhelev, D., Raycheva, L., Rangelov, N.* "INNOSEIS – Valorization of Innovative Anti-seismic Devices", Work Package 6 – Deliverable 6.2 Specifications for Device Manual, European Commission Research Programme of the Research Fund for Coal and Steel, 2017.

15. *Castiglioni, C., Calado, L.* "Low-Cycle Fatigue Behaviour and Damage Assessment of Semi-Rigid Beam-to-Column Connections in Steel", Article, IABSE reports, doi.org/10.5169/seals-56915, 1996.

16. *Bernuzzi, C., Calado, L., Castiglioni, C.* "Low-Cycle Fatigue of Structural Steel Components: a Method for Re-ananlysis of Test Data and a Design Approach Based on Ductility", ISET Journal of Earthquake Technology, Paper No. 401, Vol. 37, No. 4, 2000.

17. *Ballio, G., Castiglioni, C.* "A Unified Approach for the Design of Steel *Structures* under Low and/or High Cycle Fatigue", Journal of Construction Steel Research, Vol. 34, № 1, 1995.

18. Seismosoft, "SeismoStruct v7.0 – A Computer Program for Static and Dynamic Nonlinear Analysis of Framed Structures", available from http://www.seismosoft.com, 2014.

19. *D'Aniello, M., Ambrosino, G., Portioli, F. Landolfo, R.* "Modelling Aspects of the Seismic Response of Steel Concentric Braced Frames", Steel and Composite Structures, Vol. 15, No. 5, pp. 539-566, 2013.

20. *Georgiev, Tzv., Zhelev, D., Raycheva, L., Rangelov, N.* "INNOSEIS – Valorization of Innovative Anti-seismic Devices", Work Package 4 – Deliverable 4.1. Volume on Case Studies for Low-Rise Buildings, European Commission Research Programme of the Research Fund for Coal and Steel, 2017 *(Articles in Press).*

21. Seismomatch v.2.1.0, Seismosoft, www.seismosoft.com.

22. *Raycheva, L., Georgiev, Tzv., Ganchev, O., Raykov, S.* "Experimental Investigation of Split-X Concentrically Braced Frames" (in Bulgarian), Annual of the University of Architecture, Civil Engineering and Geodesy, Sofia, Vol. 50, 2017.

23. *Uriz, P., Mahin, S.* "Toward Earthquake-Resistant Design of Concentrically Braced Steel-Frame Structures", Pacific Earthquake Engineering Research Center (PEER) Report 2008/08, University of California, Berkeley, 2008.

ОЦЕНКА НА НАТРУПВАНЕТО НА ПОВРЕДИ ОТ УМОРА В SPLIT-X ВЕРТИКАЛНИ ВРЪЗКИ

Л. Райчева[1], Цв. Георгиев[2]

Ключови думи: *нискоциклична умора, диагонални елементи, експериментално изследване, натрупване на повреди при цикличен тест*

РЕЗЮМЕ

Настоящият доклад разглежда характерен аспект при цикличното нелинейно поведение на стоманени рамки с кръстосани диагонали, пресичащи се в междинна греда. Проведени са експериментални изследвания на три броя едноетажни едноотворни образци на стоманени рамки с диагонали с отворени напречни сечения, подложени на хоризонтално въздействие в симетрични знакопроменливи цикли с постоянна амплитуда. Проведените тестове доказват обособен механизъм на развитие на повреди в диагоналните елементи, който може да се опише с последователност от характерни стадии.

Предложено е дефиниране на характерните стадии на развитие на повредите и е изведен критерий за оценка на степента на тяхното натрупване. Експерименталните изследвания сочат, че след достигане на определено ниво на натрупани повреди в диагоналите, настъпва прогресивен спад в капацитета за дисипация на енергия на конструкцията. На база на проведените тестове е изведен аналитичен израз за оценка на издръжливостта на диагоналите на нискоциклична умора и е демонстрирано неговото приложение при динамичен нелинеен анализ.

[1] Лора Райчева, докторант, кат. „Метални, дървени и пластмасови конструкции“, УАСГ, бул. „Хр. Смирненски“ № 1, 1046 София, e-mail: raycheva_fce@uacg.bg, lora_dr@abv.bg

[2] Цветан Георгиев, доц., кат. „Метални, дървени и пластмасови конструкции“, УАСГ, бул. „Хр. Смирненски“ № 1, 1046 София, e-mail: cvgeorgiev_fce@uacg.bg